

STUDY ON THE WELD NUGGET SIZE VARIATION WITH VARIATION OF WELDING PARAMETER CHANGES FOLLOWING THE RESISTANCE SPOT WELDING PROCESS

Dan Birsan¹

¹"Dunarea de Jos" University of Galati, dbirsan@ugal.ro.

Abstract: *This paper explores the influence of weld nugget size in the context of resistance spot welding (RSW) and its direct impact on the quality of weld joints. Resistance spot welding is a widely employed joining technique in various industries, particularly in automotive and aerospace applications. The size of the weld nugget, which is the molten and fused metal region at the joint interface, is a critical parameter affecting the structural integrity and performance of welded components.*

The study investigates how variations in welding parameters, such as current, time, and electrode force, can lead to changes in the weld nugget size. Weld nugget size directly correlates with the mechanical strength and overall durability of the welded joint. In this analysis, we examine the relationship between different welding parameter combinations and their effect on the weld nugget size.

Furthermore, we evaluate the quality of weld joints produced with varying nugget sizes, considering factors such as tensile strength, fatigue resistance, and weld consistency. Understanding this relationship is essential for optimizing the resistance spot welding process, ensuring the production of reliable and high-quality welded assemblies.

Keywords: *resistance spot welding, finite element, strain*

1. Introduction

Resistance spot welding (RSW) is a widely employed and essential process in various industries, primarily the automotive, aerospace, and manufacturing sectors. It involves the joining of metal components by melting the interface through the application of heat generated by electrical resistance. The following text explores the applications of resistance spot welding in industry and the studies conducted to optimize input parameters for improved joining quality.

Resistance spot welding is applied in: automotive industry for joining various components like body panels, chassis parts, and engine components; the aerospace industry

where plays a crucial role in assembling components of aircraft, such as wing structures, landing gear, and engine mounts; electronics and electrical industry used to assemble electrical components like battery cells, circuit boards, and electrical connectors; manufacturing and construction is employed for joining metal parts in various applications, including structural components, pipelines, and metal furniture.

Optimizing the input parameters in resistance spot welding is essential to ensure high-quality, defect-free welds. Researchers and engineers have conducted numerous studies to understand the relationship between input parameters and joining quality.

Resistance spot welding is a versatile and indispensable process used in various

industries. Researchers and engineers continue to explore the relationships between input parameters and joining quality through extensive studies. These investigations have led to improved welding techniques, equipment, and control systems, ultimately enhancing the reliability and efficiency of resistance spot welding in industrial applications.

Zhao et al. [1] presents results of investigations on mechanical properties and nugget evolution in resistance spot welding of Zn–Al–Mg galvanized DC51D steel. Zn–Al–Mg coating galvanized steel in resistance spot welded (RSW) in different configurations of DC51D was investigated to illustrate the nugget evolution process and mechanical properties of the joints. The study aimed to examine the nugget development process and mechanical characteristics of joints in resistance spot welded (RSW) galvanized steel with Zn–Al–Mg coating, using various configurations of DC51D.

Ebrahimpour et al. [2] presents 3D coupled thermal-electrical-structural finite element investigation on the effect of welding parameters on the geometry of nugget zone and HAZ in RSWed TRIP steel joints. The influence of resistance spot welding (RSW) parameters – specifically, current intensity, welding time, and welding force (represented as A, B, and C) – on the dimensions of the nugget (radius, thickness, and area) and the heat-affected zone (HAZ) radius in transformed induced plasticity (TRIP) steel joints was examined using a design of experiment (DOE) approach along with response surface methodology (RSM).

Xing et al. [3] presents an optimization and improvement of the projection welding of nut based on regression analysis. The paper introduces a novel framework for predicting and analyzing welding quality through the application of regression analysis methods. By employing multiple nonlinear regression analysis, the study establishes a relationship between welding parameters (namely welding time, welding current, and electrode force) and the Pull-out load of M6 welded square nuts on 1.5 mm thick pickled hot-rolled steel. Additionally, the paper delves into a discussion

of how welding parameters impact and interact with the Pull-out load.

2. Numerical Model

When it comes to resistance spot welding, the temperature field profile is contingent upon several key factors such as voltage, amperage, and welding speed, as well as the thermo-physical properties of the base material, encompassing specific heat, thermal conductivity, thermal diffusivity, mass density, and heat dissipation through convection and radiation. To comprehensively define a resistance welding process, an enclosed electrical circuit has been established that consists of a rigid body carrying a specified electrical current and another rigid body, which maintains a defined electrical potential of 0V while being in electrical contact with the rest of the circuit. The rigid body set at 0V essentially serves as the ground, while the other rigid body functions as an electrode. The 3D finite element model comprises two plates measuring 50x50x0.8 mm each and two weld guns with copper electrodes (B0-13-18-30-5-31, following ISO 5821), as illustrated in the figure 1. The mesh is fine around these weld lines, and coarse in the far field.

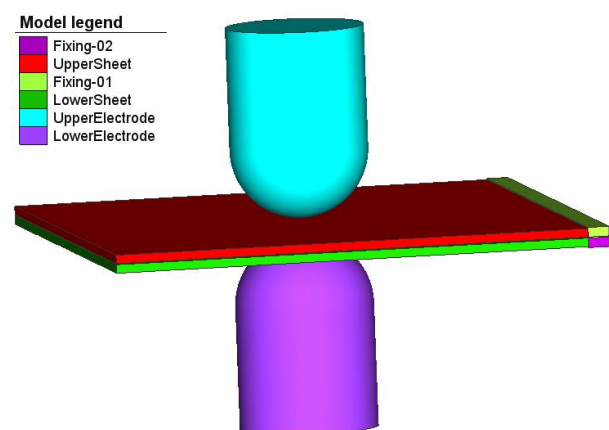


Figure 1: 3D finite elements model

The plates have been constrained with fixing in order to simulate the real physic process.

The plates were simulated using 2D elements specifically designed for the analysis of 2D axi-symmetric scenarios, referred to as Quad (10) in Simufact Forming terminology.

On the other hand, the rigid tools were represented by quadric elements known as Quad (40) [12]. The initial mesh was generated using the Advanced Front Quad mesher. However, this mesh displayed significant distortion during the welding process, leading to a divergence issue. To address this problem, an automatic rescaling technique was employed. This automated process regenerated the meshes, allowing the simulation to continue using the updated mesh configuration. In total, the upper and lower plates were modeled using 1028 elements, while all the rigid bodies (including the pin, sleeve, table, and hollow support) were represented by 2012 elements. Fig. 2 shows the electrical material resistivity of X2CrTiNb18 stainless steel.

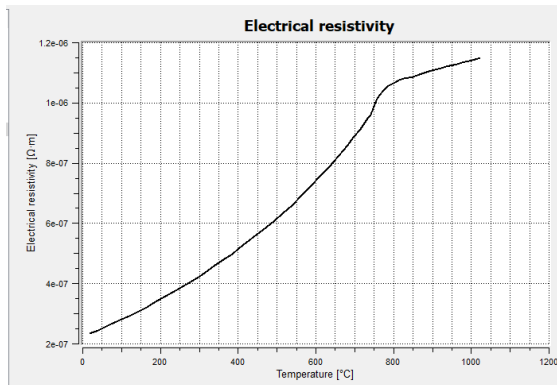


Figure 2: Definition of the electrical material resistivity

The heat transfer in the structure was modelled as 3D heat transfer problem using the Simufact Welding software. X2CrTiNb18 stainless steel has been used in this simulation and Table 1 shows the chemical composition.

Table 1: X2CrTiNb18 chemical composition (%)

Equivalent values (calculated from the composition above)			
Name	Minimum	Maximum	Fixed value
Carbon CEV	3.5	3.89667	3.70667
Carbon CET	0.875	1.055	0.9755
Carbon PCM	0.875	1.03833	0.967333
Nickel (eq Schaeffler)	0	1.4	0.8
Nickel (eq DeLong)	0	1.4	0.83
Chrome (eq)	17.67	20.62	18.97

The model incorporates two time-dependent tables: the Clamp Force Table (see Fig. 3) and the Electrical Current Table (see Fig. 4). Throughout the simulation, which has a welding time of 1.0 second, it is essential for the

Clamp Force to remain steady at 1700 Newtons. The electric current introduced into the model varied between 5000 and 5500 A with a step of 100 A and the action time is between 0.14 and 0.18 s.

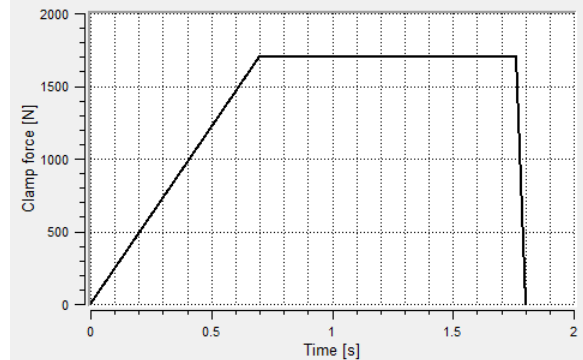


Figure 3: Clamp force during the resistance welding process

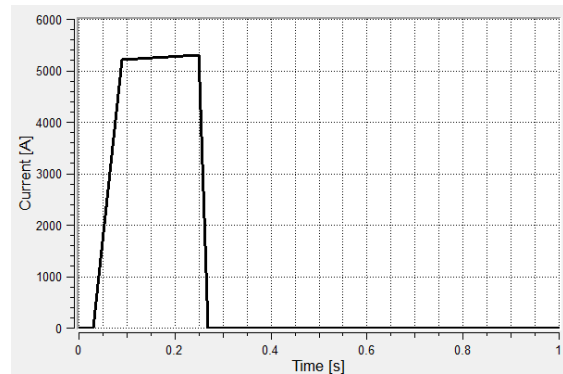


Figure 4: Electrical current during the resistance welding process

The material flow stress obtained from the material database integrated into the Simufact Forming software [12] is shown in Fig.5 and they correspond to a temperature and strain rate-dependent material model based on the MatILDa database.

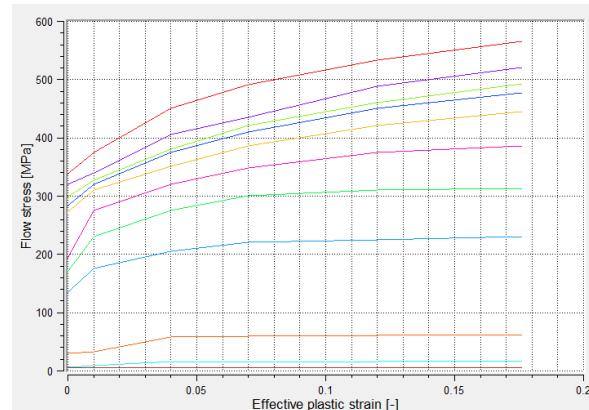


Figure 5: Variation of flow stress with temperature

3. Results

Multiple runs were conducted using various input values for both current and welding time. For each dataset, different weld nugget values were obtained, which are summarized in the following.

Table 2: Parameters to be studied

Weld time [s]	0.16
Current [A]	5000
	5050
	5100
	5150
	5200
	5250

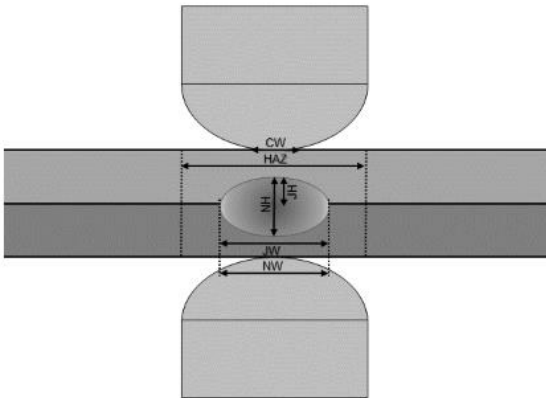


Figure 6: Nugget dimensions

Following the runs performed for the input data values from Table 2, the following values for the dimensions of the weld nugget were obtained.

For I=5000A, t=0.16s

Measuring		
Name	Variable	Value
Nugget height solidus	NH	0.528 mm
Nugget width solidus - 1st sheet	NW	1.841 mm
Nugget width solidus - 2nd sheet	NW	1.792 mm
Joint height solidus 1 - upper sheet	JH	0.0 mm
Joint height solidus 1 - lower sheet	JH	0.0 mm
Joint height solidus 2 - upper sheet	JH	0.276 mm
Joint height solidus 2 - lower sheet	JH	0.243 mm
Joint height solidus 3 - upper sheet	JH	0.447 mm
Joint height solidus 3 - lower sheet	JH	0.513 mm

For I=5050A, t=0.16s

Measuring		
Name	Variable	Value
Nugget height solidus	NH	0.53 mm
Nugget width solidus - 1st sheet	NW	1.835 mm
Nugget width solidus - 2nd sheet	NW	1.84 mm
Joint height solidus 1 - upper sheet	JH	0.0 mm
Joint height solidus 1 - lower sheet	JH	0.0 mm
Joint height solidus 2 - upper sheet	JH	0.275 mm
Joint height solidus 2 - lower sheet	JH	0.246 mm
Joint height solidus 3 - upper sheet	JH	0.446 mm
Joint height solidus 3 - lower sheet	JH	0.516 mm

For I=5100A, t=0.16s

Measuring		
Name	Variable	Value
Nugget height solidus	NH	0.651 mm
Nugget width solidus - 1st sheet	NW	2.298 mm
Nugget width solidus - 2nd sheet	NW	2.274 mm
Joint height solidus 1 - upper sheet	JH	0.332 mm
Joint height solidus 1 - lower sheet	JH	0.319 mm
Joint height solidus 2 - upper sheet	JH	0.341 mm
Joint height solidus 2 - lower sheet	JH	0.309 mm
Joint height solidus 3 - upper sheet	JH	0.472 mm
Joint height solidus 3 - lower sheet	JH	0.576 mm
Joint width solidus - 1st sheet/2nd sheet	JW	1.179 mm

For I=5150A, t=0.16s

Measuring		
Name	Variable	Value
Nugget height solidus	NH	0.672 mm
Nugget width solidus - 1st sheet	NW	2.386 mm
Nugget width solidus - 2nd sheet	NW	2.334 mm
Joint height solidus 1 - upper sheet	JH	0.34 mm
Joint height solidus 1 - lower sheet	JH	0.331 mm
Joint height solidus 2 - upper sheet	JH	0.351 mm
Joint height solidus 2 - lower sheet	JH	0.32 mm
Joint height solidus 3 - upper sheet	JH	0.47 mm
Joint height solidus 3 - lower sheet	JH	0.587 mm
Joint width solidus - 1st sheet/2nd sheet	JW	1.31 mm

For I=5200A, t=0.16s

Measuring		
Name	Variable	Value
Nugget height solidus	NH	0.737 mm
Nugget width solidus - 1st sheet	NW	2.591 mm
Nugget width solidus - 2nd sheet	NW	2.562 mm
Joint height solidus 1 - upper sheet	JH	0.37 mm
Joint height solidus 1 - lower sheet	JH	0.368 mm
Joint height solidus 2 - upper sheet	JH	0.384 mm
Joint height solidus 2 - lower sheet	JH	0.352 mm
Joint height solidus 3 - upper sheet	JH	0.625 mm
Joint height solidus 3 - lower sheet	JH	0.62 mm
Joint width solidus - 1st sheet/2nd sheet	JW	2.427 mm

For I=5250A, t=0.16s

Measuring		
Name	Variable	Value
Nugget height solidus	NH	0.749 mm
Nugget width solidus - 1st sheet	NW	2.574 mm
Nugget width solidus - 2nd sheet	NW	2.522 mm
Joint height solidus 1 - upper sheet	JH	0.377 mm
Joint height solidus 1 - lower sheet	JH	0.372 mm
Joint height solidus 2 - upper sheet	JH	0.391 mm
Joint height solidus 2 - lower sheet	JH	0.356 mm
Joint height solidus 3 - upper sheet	JH	0.633 mm
Joint height solidus 3 - lower sheet	JH	0.624 mm
Joint width solidus - 1st sheet/2nd sheet	JW	2.427 mm

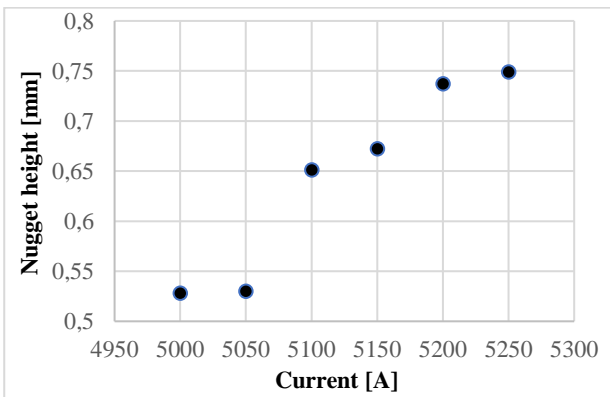


Figure 7: Nugget height vs current

The welded joints were subjected to shearing, with the upper plate moving at a speed of 1 mm/s relative to the lower plate until the joint yielded. For each case, the maximum value of plastic deformation was recorded, as shown in Fig. 8. The correlation between the size of the solid-state weld nugget and the magnitude of plastic deformation can be observed.

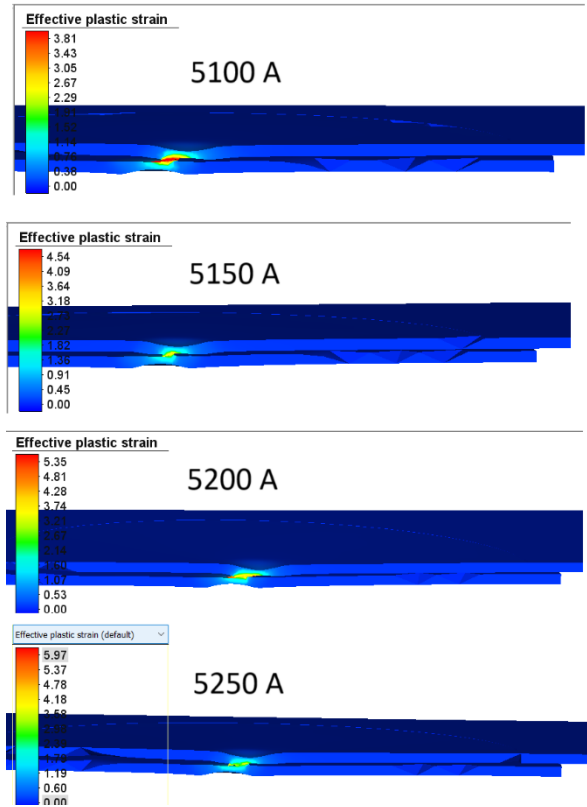


Figure 8: Effective plastic strains

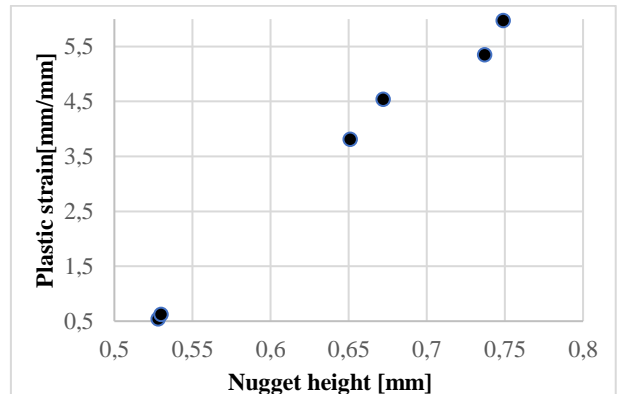
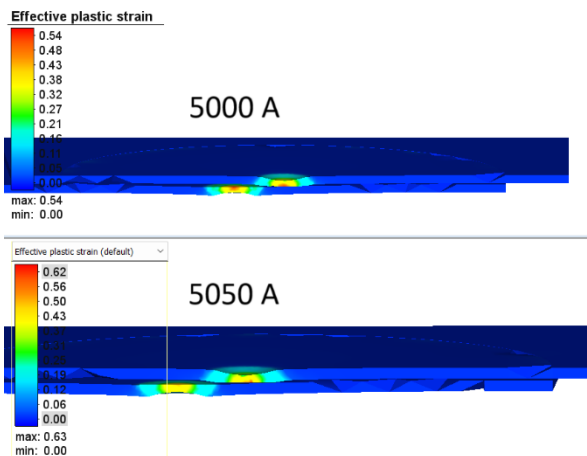


Figure 9: Effective plastic strains vs nugget height



4. Conclusions

The purpose of this study was to conduct a finite element analysis of spot resistance welding joints of stainless-steel sheets for various current values, which resulted in different sizes of the weld core. Within the same model, the welded joint was subjected to shearing, with plastic strains values increasing as the size of the solid-state welded nugget was increased.

It can be seen in Fig. 7 that, for current values of 5000 and 5050 A, the height of the weld nugget is small which means that the joint is not resistant. In Fig. 9 it can be seen that, for the above-mentioned current values, the plastic strains occurring in the joint as a result of the shearing process are very small, which means that the joint is not resistant.

References

- [Zhao, 2023] Zhao L., Lu Y., Xiong Z., Sun L., Qi J., Yuan X., and Peng J., *Mechanical properties and nugget evolution in resistance spot welding of Zn-Al-Mg galvanized DC51D steel*, Journal of High Temperature Materials and Processes, ISSN 0334-6455, 2023.
- [Ebrahimpour, 2023] Ebrahimpour A., Mostafapour A., Haggi N., *3D Coupled Thermal-Electrical-Structural Finite Element Investigation on the Effect of Welding Parameters on the Geometry of Nugget Zone and HAZ in RSWed TRIP Steel joints*, Iranian Journal of Materials Science and Engineering, Vol. 20, Number 1, ISSN 1735-0808, 2023.
- [XING, 2022] XING L., YU T., ZHANG J., XING X. and LU H., *Optimization and Improvement of the Projection Welding of Nut Based on Regression Analysis*, ISIJ International, Vol. 63 (2023), No. 4, pp. 694–702, ISSN 0915-1559, 2022.
- [Bîrsan, 2023] Bîrsan D. C., Paunoiu V., Teodor V., *Neural networks applied for predictive parameters analysis of the refill friction stir spot welding process of 6061-T6 aluminum alloy plates*, Journal of Materials, Vol. 16, Issue 13, 2023.
- [Bîrsan, 2023] Bîrsan D. C., Gurău C., Marin F. B., Ștefănescu C., Gurău G., *Modeling of severe plastic deformation by HSHPT of as cast Ti-Nb-Zr-Ta-Fe-O Gum alloy for orthopaedic implant*, Journal of Materials, Vol. 16, Issue 8, 2023.
- [Bîrsan, 2022] Bîrsan D. C., Simion G., *Numerical modelling of thermo-mechanical effects developed in resistance spot welding of E304 steel with copper interlayer*, Annals of “Dunarea de Jos” University, Fascicle XII, Welding Equipment and Technology, 2022, Vol. 33, pp. 89-94.
- [Bîrsan, 2022] Bîrsan D., *Simulation of a refill friction stir spot welding process*, New Technologies and Products in Machine Manufacturing Technologies Journal, P - ISSN-1224-029X, E - ISSN-2247-6016.
- [Bîrsan, 2021] Bîrsan D., *Thermal field and residual stresses during the resistance spot welding process*, New Technologies and Products in Machine Manufacturing Technologies Journal, P - ISSN-1224-029X, E - ISSN-2247-6016.
- [Bîrsan, 2021] Bîrsan D. C., Simion G., Voiculescu I., Scutelnicu E., *Numerical Model Developed for Thermo-Mecahnical Analysis in AlCrFeMnNiHf0.05-Armox 500 Steel Welded Joint*, Annals of “Dunarea de Jos” University, Fascicle XII, Welding Equipment and Technology, 2021, Vol. 32, pp. 37-46.
- [Florescu, 2018] Florescu S.N, Mihăilescu D., Bîrsan D.C., Mocanu C.I., *Researches on the thermal fields analysis at MAG-M mechanized butt welding with solid wire*, The Annals of Dunarea de Jos University of Galati, Fascicle XI, Shipbuilding, Year XXXIV, 2018, ISSN 1221-4620, Galati University Press.
- [Bîrsan, 2017] Bîrsan D., *Finite element analysis of residual stresses in naval structures due to multiarc welding process*, New Technologies and Products in Machine Manufacturing Technologies Journal, ISSN-2247-6016, pag. 234-242
- [***, 2019] ***, *Simufact Forming Theory manual*. Computational Applications and System Integration Inc., 2019.